

# Electrochemistry of Group VI Metal Carbonyl Compounds Containing 1,1'-Bis(diphenylphosphino)ferrocene

Amanda C. Ohs,<sup>†,‡</sup> Arnold L. Rheingold,<sup>§</sup> Michael J. Shaw,<sup>||</sup> and Chip Nataro<sup>\*,†</sup>

Department of Chemistry, Lafayette College, Easton, Pennsylvania 18042, Department of Chemistry and Biochemistry, University of California, La Jolla, California 92093, and Department of Chemistry, Southern Illinois University, Edwardsville, Illinois 62026

Received April 12, 2004

The oxidative electrochemistry of a variety of homo- and bimetallic group VI metal carbonyl compounds containing 1,1'-bis(diphenylphosphino)ferrocene (dppf) with the general formulas  $M(\text{CO})_5(\text{dppf})$  (**1a–c**),  $M(\text{CO})_4(\text{dppf})$  (**2a–c**), and  $(\text{CO})_5M(\text{dppf})M'(\text{CO})_5$  (**3a–f**) ( $M, M' = \text{Cr}, \text{Mo}, \text{W}$ ) was investigated. The effect of the group VI metal and the coordination mode of the dppf ligand on the potential at which the oxidation of the group VI metals and the ferrocene backbone of dppf occurred was examined.

## Introduction

A variety of reactions have been catalyzed using transition-metal compounds that contain the ligand 1,1'-bis(diphenylphosphino)ferrocene (dppf).<sup>1</sup> A number of reasons for the enhanced catalytic activity of these compounds have been presented: in particular, the bite angle of dppf and the redox-active ferrocene backbone.<sup>1</sup> The oxidative electrochemistry of dppf has been studied, and unlike its close relative ferrocene, the product of dppf oxidation undergoes a chemical reaction.<sup>2</sup> However, the dppf-based oxidation often becomes reversible when dppf is coordinated to a metal center, as seen in the oxidative electrochemistry of  $[\text{MCl}_2(\text{dppf})]$  ( $M = \text{Pd}, \text{Pt}$ ).<sup>3</sup> Although electrochemical studies have been performed on compounds containing a dppf ligand, none have investigated the effect of varying dppf coordination modes on the electrochemistry of the ferrocene backbone.

The most commonly found modes of dppf coordination are monodentate, bidentate, and bridging.<sup>1,4</sup> A variety of homo- and bimetallic group VI metal carbonyl compounds with varying dppf coordination modes have been prepared (Figure 1).<sup>5</sup> It is surprising that the electrochemistry of the entire series has not been explored, since this series presents dppf bound to a series of metal centers in a variety of coordination modes. In fact, only one of these compounds,  $\text{Mo}(\text{CO})_4(\text{dppf})$ , has been investigated electrochemically; the oxidation shows a

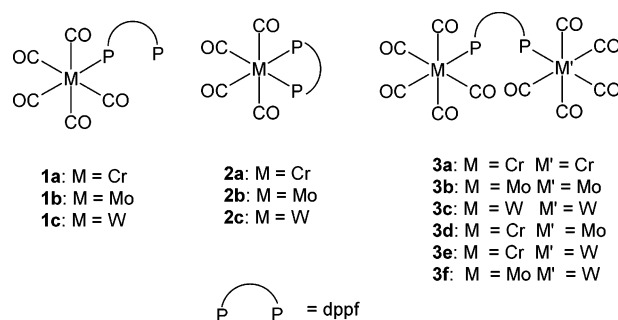


**Figure 1.** Monodentate, bidentate, and bridging coordination modes of dppf.

chemically irreversible wave at 0.42 V versus  $\text{Fc}^{0/+}$  in THF.<sup>6</sup> The effect of group VI metals on the electrochemistry of coordinated dppf has been investigated in a series of compounds,  $[\text{MCl}_n\{\mu\text{-dppf}\}M'(\text{CO})_5]_n$  ( $M = \text{Au}, M' = \text{Cr}, \text{Mo}, \text{W}, n = 1; M = \text{Pd}, \text{Pt}; M' = \text{Cr}, \text{Mo}, \text{W}, n = 2$ ).<sup>7</sup> Data from this series have shown that there does not appear to be a significant difference in the potential at which the ferrocene backbone undergoes oxidation as  $M'$  varies. However, in both series, the dppf ligand bridges two different metal centers; thus, the effect of varying coordination modes on the oxidative electrochemistry could not be examined.

The purpose of this work is to investigate how the three known coordination modes of dppf to group VI metal carbonyls and the variation of the group VI metal present influence the electrochemistry of the compound. The oxidative electrochemistry of 12 different dppf-containing compounds was examined, and the effect of the dppf coordination mode (monodentate, bidentate, or bridging) on the ferrocene-based oxidation of a dppf ligand was determined. In addition, the relationship between the coordination mode of the dppf ligand and the potential at which the oxidation of the group VI

\* To whom correspondence should be addressed. E-mail: nataroc@lafayette.edu.

<sup>†</sup> Lafayette College.

<sup>‡</sup> Current address: Department of Chemistry and Biochemistry, University of California, La Jolla, CA 92093.

<sup>§</sup> University of California.

<sup>||</sup> Southern Illinois University.

(1) (a) Gan, K. S.; Hor, T. S. A. In *Ferrocenes*; Togni, A., Hayashi, T., Eds.; VCH: New York, 1995. (b) Colacot, T. J. *Platinum Met. Rev.* **2001**, *45*, 22.

(2) Nataro, C.; Campbell, A. N.; Ferguson, M. A.; Incarvito, C. D.; Rheingold, A. L. *J. Organomet. Chem.* **2003**, *673*, 47.

(3) Corain, B.; Longato, B.; Favero, G.; Ajb, D.; Pilloni, G.; Russo, U.; Kreissl, F. R. *Inorg. Chim. Acta* **1989**, *157*, 259.

(4) Bandoli, G.; Dolmella, A. *Coord. Chem. Rev.* **2002**, *209*, 161.

(5) Hor, T. S. A.; Phang, L.-T. *J. Organomet. Chem.* **1989**, *373*, 319.

(6) DuBois, D. L.; Eigenbrot, C. W., Jr.; Miedaner, A.; Smart, J. C.; Haltiwanger, R. C. *Organometallics* **1986**, *5*, 1405.

(7) Phang, L.-T.; Au-Yeung, S. C. F.; Hor, T. S. A.; Khoo, S. B.; Zhou, Z.-Y.; Mak, T. C. W. *J. Chem. Soc., Dalton Trans.* **1993**, 165.

metal occurs was explored. During the course of this work, alternative syntheses for compounds **2a**, **3d–f**, and the related compound  $\text{Cr}(\text{CO})_4(\text{dppm})$  were developed. In addition, compounds **2a** and **3a** were characterized by spectroelectrochemistry and the structure of compound **2a** was determined by X-ray crystallography.

### Experimental Section

**General Procedures.** Preparative reactions were carried out under an atmosphere of argon using Schlenk techniques. Solvents were purified under nitrogen using standard methods. Hexanes and methylene chloride ( $\text{CH}_2\text{Cl}_2$ ) were refluxed over  $\text{CaH}_2$  and then distilled. HPLC grade  $\text{CH}_2\text{Cl}_2$ , from Aldrich, used in electrochemical measurements was refluxed over  $\text{CaH}_2$  and distilled under an atmosphere of argon. Tetrahydrofuran (THF) was distilled from potassium benzophenone ketyl. The metal hexacarbonyls, dppf, decamethylferrocene ( $\text{Fc}^*$ ), and acetylferrocene were purchased from Strem.  $\text{Cr}(\text{CO})_6$  was freshly sublimed prior to use. Tetrabutylammonium hexafluorophosphate ( $\text{NBu}_4\text{PF}_6$ ), trimethylamine *N*-oxide (TMNO), and silica gel (200–400 mesh, 60 Å) were purchased from Aldrich. Tris(4-bromophenyl)aminium hexafluorophosphate,  $[\text{N}(\text{C}_6\text{H}_4\text{Br})_3][\text{PF}_6]$ , was prepared according to the literature procedure.<sup>8</sup>

**Preparation of Compounds. Synthesis of 1a–c, 2a–c, and 3a–c.** These compounds were prepared according to literature methods with minor modifications in the purification process.<sup>5</sup> Instead of using thin-layer chromatography, purification was accomplished with column chromatography, on silica gel, using mixtures of hexanes and  $\text{CH}_2\text{Cl}_2$ .

**Alternate Synthesis of 2a.** Compound **2a** was prepared in 65% yield by the photolysis of a mixture of  $\text{Cr}(\text{CO})_6$  and dppf in THF.

**Synthesis of 3d,f.** These compounds were prepared using a slight modification of the literature synthesis.<sup>9</sup> In separate flasks, equimolar quantities of the appropriate metal hexacarbonyl were reacted with TMNO in a 3:8 mixture of  $\text{CH}_2\text{Cl}_2$  and THF. These solutions were then added to an equimolar amount of dppf in a 3:8 mixture of  $\text{CH}_2\text{Cl}_2$  and THF. Following removal of the solvent, the compounds were purified by column chromatography.

**Synthesis of 3e.** A solution of  $\text{W}(\text{CO})_6$  in THF was irradiated in a photolysis vessel with a 5.5 W mercury lamp. An equimolar amount of  $\text{Cr}(\text{CO})_6$  was similarly reacted in a second photolysis vessel. The solutions were then added to an equimolar amount of dppf in THF. The product was purified by column chromatography on silica gel.

**Synthesis of  $\text{Cr}(\text{CO})_4\text{dppm}$ .**  $\text{Cr}(\text{CO})_6$  (0.035 g, 0.16 mmol) and dppm (0.027 g, 0.071 mmol) were placed in a photochemical reaction vessel equipped with a stir bar. THF (10.0 mL) was added, and the solution was cooled by flowing cold water through a jacketed quartz immersion well. Argon was bubbled through the solution, and the reaction mixture was irradiated for 45 min using a 5.5 W mercury lamp. The solution was transferred to a Schlenk flask and stirred for 2 h. The volume was then reduced in vacuo, and the product was purified by column chromatography on silica gel. The product was eluted using a mixture of 1:10  $\text{CH}_2\text{Cl}_2$  and hexanes. This yielded 7.2 mg (26% yield) of the desired product, as confirmed by comparing the IR spectrum to the literature data.<sup>10</sup>

**Chemical Oxidation of 2a.** Acetylferrocenium hexafluorophosphate was prepared by reacting equimolar amounts (0.013 mmol) of acetylferrocene and  $[\text{N}(\text{C}_6\text{H}_4\text{Br})_3][\text{PF}_6]$  in a minimal amount of  $\text{CH}_2\text{Cl}_2$ . This solution was then added dropwise to a solution of **2a** (9.0 mg, 0.013 mmol) already

**Table 1. Crystal Data and Structure Refinement Details for  $\text{Cr}(\text{CO})_4(\text{Fe}(\text{C}_5\text{H}_4\text{PPh}_2)_2)\cdot\text{CH}_2\text{Cl}_2$**

formula	$\text{C}_{39}\text{H}_{30}\text{Cl}_2\text{CrFeO}_4\text{P}_2$
formula wt	803.32
cryst syst	triclinic
space group	$P\bar{1}$
<i>a</i> , Å	10.1832(14)
<i>b</i> , Å	10.9023(17)
<i>c</i> , Å	17.987(3)
$\alpha$ , deg	82.471(3)
$\beta$ , deg	76.908(3)
$\gamma$ , deg	84.290(3)
<i>V</i> , Å <sup>3</sup>	1923.2(5)
<i>D</i> <sub>calcd</sub> , g cm <sup>-3</sup>	1.387
<i>Z</i>	2
<i>F</i> (000)	820
cryst size, mm	0.40 × 0.30 × 0.10
<i>T</i> , K	223(2)
wavelength, Å	0.710 73
abs coeff, mm <sup>-1</sup>	0.920
$\theta$ range for data collec, deg	2.11–23.26
index ranges	$-11 \leq h \leq 5, -12 \leq k \leq 12,$ $-19 \leq l \leq 9$
no. of rflns collected	7401
no. of indep rflns	5245 ( <i>R</i> (int) = 0.0274)
abs cor	none
max and min transmissn	0.9137 and 0.7099
refinement method	full-matrix least squares on <i>F</i> <sup>2</sup>
no. of data/restraints/params	5245/0/415
goodness of fit on <i>F</i> <sup>2</sup>	1.042
final <i>R</i> indices ( <i>I</i> > 2 $\sigma$ ( <i>I</i> ))	<i>R</i> 1 = 0.0351, w <i>R</i> 2 = 0.0794
<i>R</i> indices (all data)	<i>R</i> 1 = 0.0440, w <i>R</i> 2 = 0.0808
largest diff peak and hole, e Å <sup>-3</sup>	0.446 and -0.414

dissolved in a minimum amount of  $\text{CH}_2\text{Cl}_2$ . The solution immediately turned purple and was stirred for 20 min to ensure that the reaction was complete. IR ( $\text{CH}_2\text{Cl}_2$ ):  $\nu_{\text{CO}}$  (cm<sup>-1</sup>) 2071 (m) and 1966 (m).

**Crystallography.** Crystals of **2a** were obtained by dissolving the solid in a minimum amount of  $\text{CH}_2\text{Cl}_2$ , layering the solution with hexanes, and then cooling the mixture in a freezer. Crystals were found to belong to the triclinic crystal system, and centrosymmetry was initially assumed and later demonstrated to be correct. Crystallographic data are presented in Table 1. The asymmetric unit consists of one  $\text{Cr}(\text{CO})_4\text{dppf}$  molecule and a molecule of  $\text{CH}_2\text{Cl}_2$  (electron count 41, expected 42). The latter was found to be highly disordered and treated as a diffuse electron density using the routine SQUEEZE (A. Spek, Platon Library). All non-hydrogen atoms were refined anisotropically, and hydrogen atoms were treated as idealized contributions. An absorption correction using SADABS was applied to the data. All computations used software provided by the Bruker Corp. (Madison, WI).

**Electrochemical Measurements.** Electrochemical studies were performed in 10.0 mL of  $\text{CH}_2\text{Cl}_2$  at ambient temperature using a Princeton Applied Research Model 263-A potentiostat. A three-electrode configuration was used with a 1.5 mm glassy-carbon-disk working electrode, a Pt-wire counter electrode, and a nonaqueous  $\text{Ag}|\text{AgCl}$  reference electrode separated from the solution by a fine glass frit. Prior to use, the working electrode was polished first with a 1  $\mu\text{m}$  diamond paste followed by a 1/4  $\mu\text{m}$  diamond paste; after each polishing, the electrode was rinsed with acetone. The experiments were carried out under a moisture-free argon atmosphere, and the argon was bubbled through a presaturation tube containing  $\text{CH}_2\text{Cl}_2$ . Solutions of the analyte were 1.0 mM, and  $\text{NBu}_4\text{PF}_6$  (0.1 M) was used as the supporting electrolyte. Scans were made at 50 mV/s and from 100 to 1000 mV/s at 100 mV/s increments. Normal pulse voltammetry experiments were conducted at a scan rate of 5 mV/s.

**Spectroelectrochemistry.** Fiber-optic spectroelectrochemical experiments were performed using a Bruker Tensor 27 FTIR modified with a Remspec fiber-optic infrared system equipped with a low-temperature probe and liquid-nitrogen-

(8) Ebersson, L.; Larsson, B. *Acta Chem. Scand., Ser. B* **1987**, *41*, 367. Ebersson, L.; Larsson, B. *Acta Chem. Scand., Ser. B* **1986**, *40*, 210.

(9) Hor, T. S. A.; Phang, L.-T. *Polyhedron* **1990**, *9*, 2305.

(10) Colquhoun, I. J.; Grim, S. O.; McFarlane, W.; Mitchell, J. D.; Smith, P. H. *Inorg. Chem.* **1981**, *20*(8), 2516.

cooled MCT detector. Current measurements were made, and potentials were controlled using a three-electrode system attached to an EG&G PAR 263 computer-controlled potentiostat.

In a typical experiment, the cell was set up as described in the literature with the fiber-optic waveguide bringing the IR beam to and from the electrode surface.<sup>11</sup> Supporting electrolyte (NBu<sub>4</sub>PF<sub>6</sub>, 0.40 g) and dry CH<sub>2</sub>Cl<sub>2</sub> (10.0 mL) were introduced, and the solution was degassed with a slow stream of dry, deoxygenated nitrogen for 5 min. Baselines were recorded for both the electrochemical (cyclic voltammetry, 200 mV/s) and the IR parts of the experiment. Enough sample was introduced to the cell to yield a 1.0 mM solution of analyte. Cyclic voltammograms were recorded at 200 mV/s to determine the appropriate potentials for spectroelectrochemical analysis. To obtain the difference spectra, a background IR spectrum was recorded for 1 min; the potential of the electrode was set to convert the analyte into its electrode product, and after 20 s of electrolysis, a 1 min IR scan was recorded with the potential still being applied.

## Results and Discussion

**Synthesis.** Compound **2a** was prepared photochemically from Cr(CO)<sub>6</sub> and dppf in THF at 0 °C. The syntheses of compounds **3d,f** were carried out by generating equimolar amounts of the requisite M(CO)<sub>5</sub>(thf) complexes and adding them to dppf. The literature method for preparing **3d** requires the preparation of **1b**, which is then reacted with Cr(CO)<sub>5</sub>(thf).<sup>9</sup> Similarly, **3f** is prepared from **1c** and Mo(CO)<sub>5</sub>(thf).<sup>9</sup> While the reported yields appear to be significantly greater (33% for **3d** and 26% for **3f**)<sup>9</sup> than those reported in this work, this is somewhat misleading. The yields of **1b,c** are 3% and 27%, respectively.<sup>5</sup> On the basis of the initial amount of dppf used, the overall yield of **3d** from the literature preparation is 0.9%, while that of **3f** is 7%. In addition, the literature syntheses require two purification steps, whereas our syntheses of these compounds give similar yields but require only one column.

A new photochemical synthesis of **3e** was developed, giving the product in 24% yield. This yield exceeds the literature method, which required isolation of **1a** followed by addition of W(CO)<sub>5</sub>(thf).<sup>9</sup> Our photochemical synthesis is significantly less time-consuming, requiring 2 h for the photolysis of the hexacarbonyls, as opposed to the 3.5 h required in the TMNO synthesis. Other advantages of the photochemical synthesis include the use of milligram quantities of reactants instead of grams and the need for only one column separation, rather than two.

**Structure.** During the preparation of **2a**, crystals suitable for X-ray analysis were obtained. The structure of **2a** was determined, completing the series of M(CO)<sub>4</sub>(dppf) (M = Cr, Mo, W) structures. The ORTEP diagram shows that the chromium atom adopts a distorted-octahedral geometry (Figure 2). The P(1)–Cr–P(2) angle is 96.67(3)°, which is significantly larger than the analogous angle in the molybdenum (95.28(2)°)<sup>12</sup> and tungsten (95.24(5)°)<sup>13</sup> derivatives. In addition, a variety of bonding parameters typically reported for dppf-containing compounds are presented for the entire series of M(CO)<sub>4</sub>dppf compounds in Table 2.

All of the dppf ligands for this series of compounds are synclinal staggered, which is defined as having a  $\tau$  angle between 25 and 45°. <sup>1a,4</sup> This arrangement is the most common configuration for  $\eta^2$  mononuclear dppf-

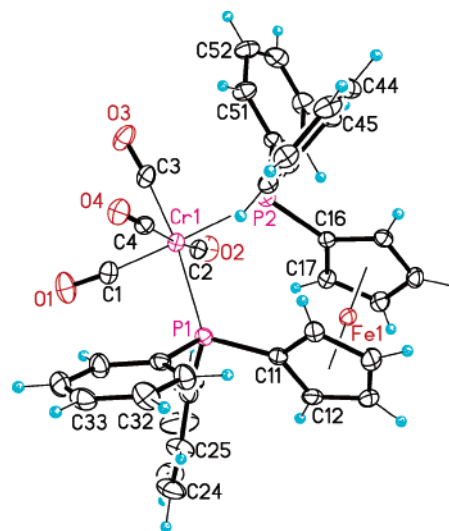


**Figure 2.** ORTEP diagram of **2a** with ellipsoids drawn at the 30% probability level. Select bond distances (Å) and angle (deg): Cr–P(1) = 2.4393(9), Cr–P(2) = 2.3984(9), Cr–C (av) = 1.864, C–O (av) = 2.306; Cr–C–O (av) = 174.0.

**Table 2.** Parameters of dppf Coordination in M(CO)<sub>4</sub>dppf (M = Cr, Mo, W)

	Cr	Mo	W
ref	this work	12	13
P–M–P (deg)	96.67(3)	95.28(2)	95.24(5)
X <sub>A</sub> –M'–X <sub>B</sub> <sup>a</sup> (deg)	179.6	179.03	178.54 <sup>d</sup>
P–Fe–P (deg)	64.02	67.32	66.94 <sup>d</sup>
$\tau^b$ (deg)	36	41.9	40.7 <sup>d</sup>
av P–M (Å)	2.4189	2.560	2.5480
P–P (Å)	3.614	3.784	3.764 <sup>d</sup>
av $\delta_P^c$ (Å)	0.042	0.022	0.049 <sup>d</sup>

<sup>a</sup> centroid–Fe–centroid. <sup>b</sup> The torsion angle C<sub>A</sub>–X<sub>A</sub>–X<sub>B</sub>–C<sub>B</sub>, where C is the carbon bonded to the P and X is the centroid. <sup>c</sup> Deviation of the P atom from the Cp plane, a positive value meaning the P is closer to Fe. <sup>d</sup> Determined from the published structural data using ORTEP-3 for Windows.<sup>23</sup>

containing compounds.<sup>1a,4</sup> The ideal  $\tau$  angle for the synclinal staggered conformation is 36°,<sup>4</sup> which is the angle found for **2a**. This ideal angle has never been seen in a pseudo-octahedral compound and has only been reported in two other structures, both of which are pseudo square planar.<sup>14</sup> It is interesting that **2a** exhibits an ideal  $\tau$  angle and yet exhibits the greatest distortion of the group VI metal center from the ideal octahedral geometry.

**Electrochemistry.** Cyclic voltammetry was used to determine the potential at which oxidation occurs for the complexes. The decamethylferrocene (Fc<sup>\*</sup>)/decamethylferrocenium (Fc<sup>\*+</sup>) couple was used as an internal standard in all measurements, because the ferrocene (Fc) couple overlaps the range of potentials for the compounds studied. All potentials were referenced to Fc/Fc<sup>+</sup> by subtracting 0.55 V from the potentials refer-

(11) Shaw, M. J.; Henson, R. L.; Houk, S. E.; Westhoff, J. W.; Jones, M. W.; Richter-Addo, G. B. *J. Electroanal. Chem.* **2002**, *534*, 47.

(12) Butler, I. R.; Cullen, W. R.; Kim, T. J.; Rettig, S. J.; Trotter, J. *Organometallics* **1985**, *4*, 972.

(13) Song, L. C.; Liu, J. T.; Hu, Q. M.; Wang, G. F.; Zanello, P.; Fontani, M. *Organometallics* **2000**, *25*, 5342.

(14) (a) Longato, B.; Pilloni, G.; Valle, G.; Corain, B. *Inorg. Chem.* **1988**, *27*, 956. (b) Vasapollo, G.; Toniolo, L.; Cavinato, G.; Bigoli, F.; Lanfranchi, M.; Pellinghelli, M. A. *J. Organomet. Chem.* **1994**, *481*, 173.

**Table 3. Potentials (V) at 100 mV/s for the Oxidation of Compounds 1a–c, 2a–c, and 3a–f vs  $Fc^{0/+}$  <sup>a</sup>**

compd	$E^{\circ}$ (Fe)	$i_r/i_f$	$E_p$	$i_r/i_f$	$E_p$	$i_r/i_f$
<b>1a</b>	0.33	0.86	0.90			
<b>1b</b>	0.32	0.75	1.02			
<b>1c</b>	0.34	0.81	1.00			
<b>2a</b>	0.35	0.99	0.21	0.96		
<b>2b</b>	0.33	0.99				
<b>2c</b>	0.37	0.93				
<b>3a</b>	0.50	0.99	0.92	1.02		
<b>3b</b>	0.51	0.68	1.05			
<b>3c</b>	0.52	0.48	1.09			
<b>3d</b>	0.50	0.74	0.98		1.29	
<b>3e</b>	0.51	0.65	1.03		1.35	
<b>3f</b>	0.52	0.68	1.05		1.38	

<sup>a</sup> All data were obtained from 1.0 mM solutions of the compound in  $CH_2Cl_2$  with 0.1 M  $NBu_4PF_6$  as the supporting electrolyte.

enced to  $Fc^*/Fc^{*+}$ .<sup>15</sup> The potentials at which oxidation occurs were measured for each compound and are listed in Table 3.

There were two waves in the oxidative electrochemistry of the  $\eta^1$  compounds (**1**). The wave at the less positive potential was assigned as a dppf-based oxidation, while the second wave was assigned as oxidation of the group VI metal. The potential at which the oxidation of the coordinated dppf in **1** occurs is shifted by approximately +0.1 V as compared to free dppf. This shift is significantly less than the shift seen in  $[MCl_2(dppf)]$  ( $M = Pd, Pt$ ), which is approximately 0.4 V.<sup>3</sup> For all three compounds, the second wave was irreversible at all scan rates employed. The first wave was reversible if the potential was switched prior to reaching the second wave but was not completely reversible when the second wave was scanned.

The oxidations of the group VI metals of **1** occur at approximately 1 V and have peak currents similar to those of the dppf-based waves. The potentials are less positive than those of the corresponding metal hexacarbonyls but significantly more positive than for other  $M(CO)_5PR_3$  compounds. In  $CH_3CN$ , the oxidation of  $Cr(CO)_5PMe_3$  occurs at 0.62 V in  $CH_3CN$ , while that of  $Cr(CO)_6$  is 1.1 V.<sup>16</sup> The chromium-based oxidation of **1a** is anticipated to be less positive than that of  $Cr(CO)_6$ , since an electron-withdrawing CO ligand is replaced by an electron-donating phosphine ligand. However, the potential was shown to be significantly more positive than for other  $Cr(CO)_5PR_3$  compounds, which can be rationalized two ways. First, dppf is not as donating as other phosphines.<sup>17</sup> The second possibility is that the dppf-based oxidation occurs prior to the group VI metal oxidation and the  $dppf^+$  ligand is anticipated to be an even weaker donor than dppf. A similar trend was noted in the oxidative electrochemistry of  $M(CO)_5(FcPh_2P)$  ( $M = Cr, Mo, W$ ) where the Fc group of the phosphine is oxidized prior to the group VI metal.<sup>18</sup>

In the series of  $\eta^2$  compounds, the oxidative electrochemistry of the chromium compound (**2a**) is quite different from that of the molybdenum (**2b**) and tung-

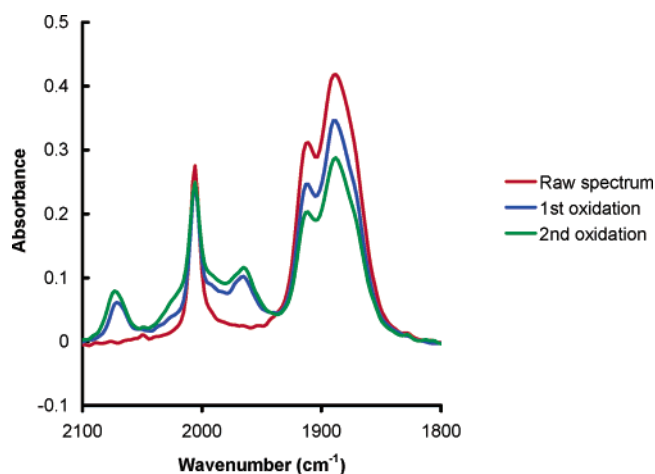


**Figure 3.** IR spectra after electrochemical oxidation of **2a**. The spectra were obtained using  $NBu_4PF_6$  (0.1 M) as the supporting electrolyte in 10.0 mL of  $CH_2Cl_2$ . Cyclic voltammograms were recorded at 200 mV/s with a 1.0 mM solution of the analyte.

sten (**2c**) analogues. There are two reversible waves in the oxidation of **2a**, and they have similar peak currents. From normal pulse voltammetry data the slope of the plot of  $E$  vs  $\log((I_d - I)/I)$  is expected to be 59 mV/n, and for the first wave the slope was determined to be 63 mV, indicating a one-electron process.<sup>19</sup> The first wave occurs at a potential considerably lower than that observed for other dppf-containing compounds in this study; however, the second oxidation is within the range of the potentials observed for the dppf-based oxidations of the other compounds. Therefore, it was essential to assign the oxidation waves in **2a**.

To assign the waves, spectroelectrochemical measurements were performed on **2a** (Figure 3). When the potential is set more positive than the first oxidation, peaks at 2063 and 1961  $cm^{-1}$  appear, while peaks at 2055 and 1882  $cm^{-1}$  diminish. This shift of approximately 65  $cm^{-1}$  is characteristic of oxidation of a metal with carbonyl ligands.<sup>20</sup> When the potential is set more positive than the second oxidation, no significant change is seen in the IR spectrum. Further support for the first oxidation being chromium-based comes from the chemical oxidation of **2a** with acetylferrocenium hexafluorophosphate, which was chosen since it undergoes oxidation at a potential (0.27 V) between the first and second waves of **2a**.<sup>21</sup> After the chemical oxidation of **2a**, new  $\nu_{CO}$  bands were observed in the IR spectrum at 2063 and 1666  $cm^{-1}$ , similar to the observations made during the spectroelectrochemical experiment.

The electrochemistry of an analogous compound,  $Cr(CO)_4(dppm)$ , was studied as additional support for the first oxidation being chromium-based.  $Cr(CO)_4(dppm)$  exhibits one chromium-based oxidation wave at 0.22 V. In addition, the shifts in the IR spectrum of  $Cr(CO)_4(dppm)^+$  compared to  $Cr(CO)_4(dppm)$  should be similar to those of  $2a^+$  versus **2a** if the first oxidation of **2a** is occurring at the chromium center. The IR

(15) Camire, N.; Mueller-Westerhoff, U. T.; Geiger, W. E. *J. Organomet. Chem.* **2001**, *823*, 637.

(16) Bond, A. M.; Carr, S. W.; Colton, R.; Kelly, D. P. *Inorg. Chem.* **1983**, *22*, 989.

(17) O'Connor, A. R.; Nataro, C. *Organometallics* **2004**, *23*, 615.

(18) Kotz, J. C.; Nivert, C. L.; Lieber, J. M. *J. Organomet. Chem.* **1975**, *91*, 87.

(19) For reversible reactions at slow scan rates, this approach is valid. Bard, A. J.; Faulkner, L. R. In *Electrochemical Methods: Fundamentals and Applications*, 2nd ed.; Wiley: New York, 2001; p 282.

(20) Camire, N.; Nafaddy, A.; Geiger, W. E. *J. Am. Chem. Soc.* **2002**, *124*, 7260.

(21) Connelly, N. G.; Geiger, W. E. *Chem. Rev.* **1996**, *96*, 7.

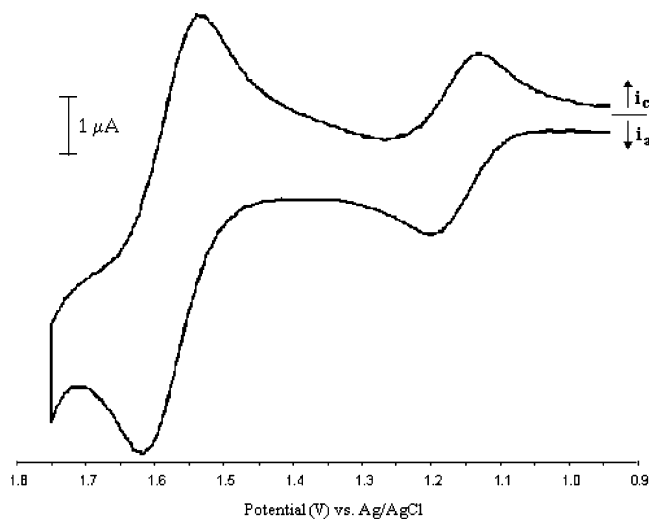


**Figure 4.** Cyclic voltammogram of **3a** measured at 100 mV/s in a 1.0 mM solution of the analyte in  $\text{CH}_2\text{Cl}_2$  with  $\text{NBu}_4\text{PF}_6$  (0.1 M) as the supporting electrolyte.

spectrum of  $[\text{Cr}(\text{CO})_4(\text{dppm})][\text{BF}_4]$  has been reported, and the peaks shift by approximately  $70\text{ cm}^{-1}$ ,<sup>22</sup> similar to spectroelectrochemical and chemical oxidation of **2a**. On the basis of these studies it can be concluded that the first wave in the oxidation of **2a** is chromium-based and the second is dppf-based.

The oxidative electrochemistry of **2b** has previously been examined and was reported to be irreversible.<sup>6</sup> In this study the oxidation of **2b** was found to be reversible. The differences in the reversibility are most likely due to the solvent used in each analysis. The earlier study used THF, which is a much more coordinating solvent than  $\text{CH}_2\text{Cl}_2$ .  $\text{Mo}(\text{CO})_6$  has a shown tendency to form a seven-coordinate intermediate; therefore, it is likely that the irreversibility reported for the oxidation of **2b** in THF is due to the formation of a highly reactive seven-coordinate intermediate.<sup>18</sup> Similar to this study, the previous study of the oxidation of **2b** found only one oxidation wave.<sup>6</sup> Since the potentials in **2b,c** are similar to that of the dppf-based oxidation in **2a**, it is likely that these are dppf-based oxidations. It is unclear why there are no waves observed for the group VI metal.

Finally, the oxidative electrochemistry of the bridging species (**3**) was investigated. The cyclic voltammogram of compound **3a** (Figure 4) exhibits unusual behavior in this series of compounds, since it displays two reversible oxidations. The second wave in the cyclic voltammogram of **3a** has a peak current approximately twice the magnitude of the first wave. Using the plots of  $E$  vs  $\log((I_d - I)/I)$  from normal pulse voltammetry, the first wave had a slope of 60 mV (a one-electron process) and the second wave had a slope of 120 mV (a two-electron process). On the basis of the oxidative electrochemistry of dppf and the metal hexacarbonyl complexes, there are three redox-active metal centers in **3a**. To assign the two waves to the appropriate metal center, **3a** was studied using spectroelectrochemistry.

A solution of **3a** was placed in the electrochemical cell and the potential set more positive than the first oxidation wave. The IR spectrum was then obtained,

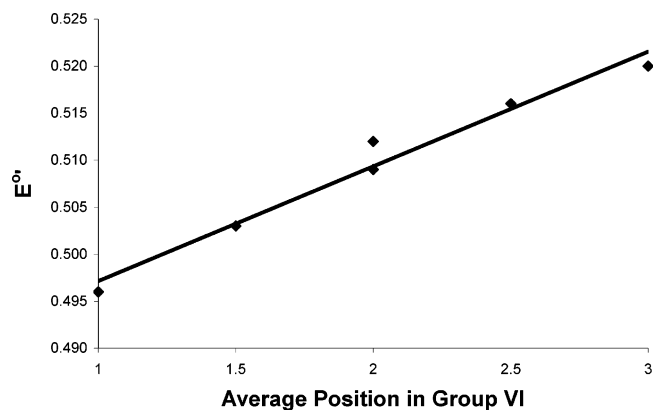


**Figure 5.** Plot of  $E'$  values of the ferrocene-based oxidation ( $R^2 = 0.971$ ) for compounds **3a–f** versus the average position of the metals in group VI.

and no significant shift in the  $\nu_{\text{CO}}$  bands was observed. However, when the potential was set more positive than the second oxidation, a shift of about  $71\text{ cm}^{-1}$  was observed in the  $\nu_{\text{CO}}$  bands. This magnitude of shift is characteristic of an oxidation of a metal with carbonyl ligands.<sup>20</sup> These results, along with the amplitude of the waves, are indicative of the first wave being dppf-based and the second being chromium-based.

Since the potential for the first wave in **3b–f** is similar to that of **3a**, it is likely that the first wave in **3b–f** is due to oxidation of the dppf ligand and the remaining wave(s) are due to oxidation of the group VI metal. The dppf oxidation of **3b–f** is reversible if the waves at higher potential are not scanned. The group VI metal oxidations of **3a–c** occur at approximately 1 V, which is similar to the potential at which the group VI metals for **1a–c** undergo oxidation. The similar potentials of **1a** and **3a**, as well as the simultaneous oxidation of both chromium centers, imply that the group VI metal centers in **3a** are electrochemically isolated. However, this apparent electrochemical isolation is not observed in the asymmetric systems, **3d–f**. There appears to be a positive shift in the potential at which the group VI metal centers are oxidized in comparing **3d–f** to the symmetric compounds **3a–c**. This could be due to the formation of a dication prior to the final oxidation of **3d–f**, whereas in **3a–c**, two simultaneous one-electron oxidations of the monocation occur.

In this series of compounds, there are two separate points to consider. The first is the effect of changing the group VI metal on the potential at which the ferrocene backbone is oxidized. For a given coordination mode, the group VI metal seems to have a minimal impact on the ferrocene-based oxidations. A similar observation was made in the oxidative electrochemistry of a series of tungsten and molybdenum compounds with monodentate ferrocenylphosphines ( $\text{FcPh}_2\text{P}$ ,  $\text{Fc}_2\text{PhP}$ , and  $\text{Fc}_3\text{P}$ ).<sup>18</sup> The second consideration is the effect of the coordination mode on the potential at which oxidation occurs. In comparison to **1a** and **3a**, **2a** has the fewest carbonyl ligands and the most phosphorus donors coordinated to the group VI metal center. Therefore, it is not surprising that the oxidation of **2a** occurs at the least positive potential for the chromium center in the series. A

(22) Ashford, P. K.; Baker, P. K.; Connely, N. G.; Kelly, R. L.; Woodley, V. A. *J. Chem. Soc., Dalton Trans.* **1982**, 477.

(23) Farrugia, L. J.; *J. Appl. Crystallogr.* **1997**, 30, 565.

similar effect can be seen when comparing Mo(CO)<sub>5</sub>(FcPh<sub>2</sub>P) and Mo(CO)<sub>4</sub>(FcPh<sub>2</sub>P)<sub>2</sub>, in which the addition of another ferrocenylphosphine group causes the molybdenum oxidation to be shifted approximately 0.4 V less positive.<sup>18</sup> The dppf-based oxidations for **3a–f** are significantly different than those observed for **1a–c**, with a shift to more positive potentials of more than 0.1 V. This is due to the presence of two withdrawing metal centers bound to the dppf ligand.

Trends between electrochemistry, dppf coordination mode, and the group VI metal center were explored. For compounds **1a–c** and **2a–c**, the dppf-based oxidations occur at approximately the same potentials for the chromium and molybdenum compounds and slightly more positive for the tungsten compounds. A similar trend is noted in the potentials for the dppf-based oxidation of [(OC)<sub>5</sub>M(μ-dppf)]<sub>2</sub>M'Cl<sub>2</sub> (M = Cr, Mo, W; M' = Pd, Pt).<sup>7</sup> The potentials for dppf-based oxidation of **3a–c** become more positive on going down group VI. This opposes the trend seen in (OC)<sub>5</sub>M(μ-dppf)AuCl (M = Cr, Mo, W),<sup>7</sup> but it is unclear why this difference occurs. The dppf-based oxidations of **3d–f** occur at potentials similar to those for the symmetric compounds **3a–c**. A plot of the potentials for the dppf-based oxidations vs the average position of the group VI metal(s) shows that the potential of the asymmetric dimers is approximately the average of those of the parent symmetric dimers (Figure 5). For all of the compounds the dppf-based oxidation is most positive when the dppf

is bridging two metal centers and least positive when bound in an η<sup>1</sup> coordination mode.

### Conclusion

The electrochemistry of a series of group VI metal carbonyl compounds containing dppf in a variety of coordination modes has been investigated. Compounds **1a–c**, **2a**, and **3a–c** exhibit two oxidation waves, while compounds **2b** and **2c** display one wave and **3d–f** show three waves. Spectroelectrochemistry and chemical oxidation methods were employed to assign the waves to either the ferrocene backbone or the group VI metal. With the exception of **2a** the wave(s) at more positive potential(s) is assigned to the group VI metal(s).

**Acknowledgment.** A.C.O. and C.N. wish to thank the donors of the Petroleum Research Fund, administered by the American Chemical Society, for partial funding, the Academic Research Committee at Lafayette College for partial funding, and the Kreske Foundation for the purchase of the Joel Eclipse 400 NMR. M.J.S. wishes to thank the NSF for support (Grant No. 0213297).

**Supporting Information Available:** Full tables of crystal data, atomic coordinates, thermal parameters, and bond lengths and angles for **2a** as a CIF file and text giving details of the syntheses of **2a** and **3d–f**. This material is available free of charge via the Internet at <http://pubs.acs.org>.

OM049735T